Atmospheric Research 249 (2021) 105313

Contents lists available at ScienceDirect

Atmospheric Research

journal homepage: www.elsevier.com/locate/atmosres

Unraveling the characteristics of precipitation microphysics in summer and winter monsoon over Mumbai and Chennai – the two urban-coastal cities of Indian sub-continent

Kaustav Chakravarty [a,*], Rupali Bhangale [b], Saurabh Das [c], Prafull Yadav [a], B.A.M. Kannan [d], G. Pandithurai [a]

[a] Indian Institute of Tropical Meteorology, Ministry of Earth Sciences, India
[b] Department of Atmospheric and Space Science, Savitribai Phule Pune University, Pune, India
[c] Indian Institute of Technology, Indore, India
[d] India Meteorological Department, Ministry of Earth Sciences, India

A B S T R A C T

The characteristic features of inter-seasonal variability of precipitation microphysics for the year 2019 over Mumbai and Chennai – the two urban-coastal cities of Indian sub-continent have been studied in this paper. The importance of choosing the regions lies in the fact that these two cities are well-known for the occurrences of severe rainfall events due to the effect of south-west and north-east monsoon during the summer and winter season of Indian sub-continent respectively. It has been observed that raindrops of diameter 2-–4 mm dominate the summer rainfall over Chennai with respect to winter rainfall. Correspondingly, while comparing the two cities together, the impact of the south-west and north-east monsoon in conjunction with the interplay of the continental and maritime effect on the microphysics of precipitation over these cities is strongly visible in the analysis. The study reveals that the rainfall evolving from the continental clouds along with contrasting surface temperature produces distinct diurnal variation for the summer (winter) rainfall over Chennai (Mumbai) while such variations are not visible for the maritime clouds. It has been observed that the drops of larger diameter along with higher radar reflectivity dominated the summer rainfall of Chennai with respect to Mumbai. While for the winter rainfall, such distinct variations are visible only for higher rainfall regimes from 16 mm/h and above where the domination of larger drops is visible for the Mumbai rainfall. Thus the difference in surface temperature which in turn escalates the convective environment in the atmosphere can be termed as one of the important factors responsible for this inter-seasonal variability of precipitation microphysics.

1. Introduction

A major population of the world resides in the coastal cities due to its tactical advantages of tropical climate along with the convenient trade opportunities through sea-route. The cities being located in the coast experiences a heterogeneous behaviour of precipitation pattern in addition to high risk of flooding. It has been found from the literature that geographical features of the coastline play a vital role for the convection and rainfall over these cities (Pielke, 1974; Holland and Keenan, 1980; Simpson et al., 1993; Baker et al., 2001). Correspondingly, the interaction of land-sea bridge circulations and orographically generated winds also modulates the precipitation pattern for these places. Overall it has been observed that all these systems do exhibits a strong impact on the diurnal variation of precipitation for these coastal cities. Literature reveals that the feature of diurnal variation, which also portrays the mechanism that drives the local climate, has been thoroughly studies in various parts of the world. The peak of convective activity in the afternoon hours has been reported by Iwasaki et al. (2008) from a semi-arid region of Mongolia and by Chen et al. (2015) from the coastline of Pearl River Delta in China. By using hourly rainfall data of 90 stations of UK from 1998 to 2015, Xiao et al. (2018) reported an early morning and the late afternoon peaks of rainfall occurrences which are contributed by the frequency (the early morning) and the intensity (the late afternoon) of rainfall separately. By taking 8 years Tropical Rainfall Measuring Mission (TRMM) data, Yang and Smith (2008) suggested that these diurnal modes largely arise from distinct diurnal stratiform variations modulating convective ones. They also pointed out that the oceanic (continental) convective rainfall is up to 25% (50%) greater during nighttime (daytime) than daytime (nighttime). Thus all the studies as obtained from the literature reveals that rainfall generally starts to develop over the coastal cities in the afternoon hours, reaches its peak in the late evening hours and finally proliferate towards the ocean in the night, thereby producing an early-morning rainfall over the adjacent ocean (Kousky, 1980; Geotis and Houze, 1985; Yang and Slingo, 2001;

* Corresponding author at: Indian Institute of Tropical Meteorology, Ministry of Earth Sciences, Dr Homi Bhabha Road, Pashan, Pune 411008, India.
E-mail address: kaustav@tropmet.res.in (K. Chakravarty).

https://doi.org/10.1016/j.atmosres.2020.105313
Received 19 June 2020; Received in revised form 17 September 2020; Accepted 12 October 2020
Available online 16 October 2020

Rauniyar and Walsh, 2013; Bergemann and Jakob, 2016). In addition to the land-sea breeze interaction in the coast lines, the urban heat island effect also had a strong impact on the rainfall pattern especially over the densely populated urban coastal cities. It is well known that as the air over the city starts to get heated, it rises faster thereby creating a thermal gradient between the city and the surrounding rural areas. The convergence generated through this process enhances the rising of air mass over the city. At the same time, it is also known that the urban emission generates aerosols/pollutions which in turn increase the production of cloud condensation nuclei (CCN). Thus, the upward lifted air which also contains aerosol within it triggers the formation of clouds that ultimately fall down on the surface as heavy rainfall. As such, the temperature variations in the cities also play a vital role for the precipitation pattern over the areas.

Along with temperature, another important variability in urban-rainfall modification is due to aerosol. It has been found that the air pollution produced by industrial and urban regions catalyzes for the reduction of precipitation in different cloud systems over various regions of the world (Ramanathan et al., 2001; Rosenfeld, 2000; Jirak and Cotton, 2006). Correspondingly, it has also been observed that for some urban areas, the Giant Cloud Condensation Nuclei (GCCN) enhances the warm rain process which in turn increases the surface precipitation around urban regions (Feingold et al., 1999; Yin et al., 2000). This contrasting behaviour of aerosol for the precipitation initiation/reduction remains a challenge as the validity of the cloud invigoration effect by aerosol loading and the possibility of climate responses to this effect are still considered to be an open question in the meteorological community (Altaratz et al., 2014).

With the above background, the present study tried to highlight the microphysical features of the precipitation pattern over the urban-coastal cities of Mumbai and Chennai, which lies on the western and eastern coast of Indian sub-continent respectively. The rainfall over these two cities which are mainly contributed by the south-west and north-east monsoon, also behaves differently over these regions during the inter-seasonal period. The south-west monsoon which is also known as Indian summer monsoon generally starts in the month of June and fades away in the end of September. The moisture-laden winds from the ocean on reaching the southernmost point of the Indian Peninsula, due to its topography, become divided into two parts: the Arabian Sea Branch and the Bay of Bengal Branch. The city of Mumbai receives heavy rainfall during June to September from this Arabian Sea branch of monsoon. Correspondingly, in the month of October, the cold wind from the northern India while retreating back towards the Indian ocean, picks up moisture from Bay of Bengal which ultimately results for heavy rainfall over the southern-eastern part of Indian sub-continent during the period from October-December which are known as north-east monsoon or winter monsoon. Thus the cities like Chennai that get less rain from the southwest monsoon, receives severe rainfall from this north-east monsoon. Unlike the south-west monsoon, the study related to the variability pattern of north-east monsoon has received less importance due to its small contribution for the annual rainfall of India with 11% (Rajeevan et al., 2012). Literature reveals that the north-east monsoon rainfall displays significant variations at intraseasonal (Rajeevan et al., 2012; Dimri et al., 2016), interannual (Kripalani and Kumar, 2004; Sreekala et al., 2012; Rajeevan et al., 2012) and longer time scales (Zubair and Ropelewski, 2006; Kumar et al., 2007). Correspondingly, it has been noted that climate models have difficulty for accurately simulating the mean state and the variability of the north-east monsoon rainfall (Rodwell, 2005; Siew et al., 2014). For example, Rajeevan et al. (2012) indicated in an analysis that the seasonal rainfall hindcasts from the ENSEMBLES coupled models possess very poor skill in predicting the inter-annual variability of north-east monsoon. Similarly, Siew et al. (2014) showed that most of the models in phase 5 of the Coupled Model Intercomparison Project (CMIP5) had a significant bias of the Southeast Asian winter monsoon precipitation. As such, the proper representation of the model can be achieved if the accurate observation of rainfall estimation or rainfall microphysics can be incorporated in the models for these monsoon phases. One of the methods for getting the accurate observation of rainfall microphysics is through raindrop size distribution (DSD) as rain rate is directly proportional to the third power of rain drop diameter. Literatures reveal that raindrops vary in space and time and over a wide range of scales (e.g., Jameson et al., 2015; Jung et al., 2012; Marzano et al., 2010; Marzuki et al., 2013; Tapiador et al., 2010; Tokay and Bashor, 2010; Uijlenhoet et al., 2003; Zwiebel et al., 2015). Characteristics of DSDs in a few maritime locations are also reported in the Tropical Ocean and Global Atmosphere Coupled Ocean-Atmosphere Response Experiment carried out in Pacific (Atlas et al., 1999) and the research on the summer season DSD differences between Palau and Taiwan in western Pacific reported by Seela et al. (2017). Comparative studies on the DSD variability between maritime and continental precipitation have also been reported (Bringi et al., 2003; Rosenfeld and Ulbrich, 2003; Ulbrich and Atlas, 2007), which found lower mass-weighted mean diameter values in the maritime-like rain cluster than the continental-like rain cluster. Many studies have also elucidated the variability of DSD in different rain types and rainfall regimes (e.g., Maki et al., 2001; Moumouni et al., 2008; Thurai et al., 2010; Tokay and Short, 1996; Yuter and Houze, 1997). Correspondingly, modeled DSD parameters also play a key role in active and passive satellite-based microwave sensor rainfall estimation. For instance, three-parameter gamma distribution has been used in the rainfall estimation algorithms of Tropical Rainfall Measuring Mission (TRMM) precipitation radar (Iguchi et al., 2000; Kozu et al., 2009; Kozu et al., 2009) and in Global Precipitation Measurement Dual-frequency Precipitation Radar (Hou et al., 2008; Liao et al., 2014; Nakamura and Iguchi, 2007). Studies are also available related to the variation of raindrop size distribution over several places of India which differ widely in their climatic and topographic condition. Chakravarty et al. (2013) and Chakravarty and Raj (2013) highlighted that raindrops during pre-monsoon and post-monsoon months dominates the monsoon rainfall over Kolkata and Pune respectively. The raindrops through its distribution also shows interesting features for the orographic regions of Western Ghat (Das et al., 2017; Sumesh et al., 2019) and for the south-western coastal station of Indian peninsula (Harikumar et al., 2009; Lavanya et al., 2019; Jash et al., 2019). Variation of DSD due to maritime and continental wind was also investigated by Das and Chatterjee (2018) for a coastal location of India. Along with the above variations, several researchers in the past have highlighted the difference of raindrop size distribution during the two types of monsoon- that is the south west monsoon and north-east monsoon. Reports over Gadanki, a station situated on the leeward side of the eastern ghat mountain highlighted that the smaller drop concentration is higher in the northeast monsoon (NEM) than in the southwest monsoon (SWM) for the same rain rate. By looking into the low level winds, cloud effective radius from satellite data and the mass-weighted mean diameter from raindrop diameter the authors pointed out that the microphysical and dynamical processes related to evaporation and convection of raindrops seem to play an important role in modifying the DSD (Narayana Rao et al., 2001; Radhakrishna et al., 2009; Radhakrishna and Rao, 2010).

Keeping in view of the above studies, the initial part of the paper tried to focus on the diurnal and inter-seasonal variability of raindrop size distribution (DSD) over Chennai for the year 2019. Through this analysis, the paper also highlighted the impact of the maritime and continental clouds on the microphysics of precipitation over Chennai during the monsoon (also known as summer monsoon) and post-monsoon (also known as winter monsoon) months. The later part of the paper portrays the comparative study of the precipitation microphysics of two urban-coastal stations, that is Mumbai and Chennai as both the stations are situated opposite too each other on the coast of Arabian sea and Bay of Bengal respectively. It is very interesting to note that Chennai act as the leeward (windward) side of the south-west monsoon (north-east monsoon) whereas Mumbai behaves completely opposite with respect to Chennai as it acts the windward (leeward) side

for the south-west monsoon (north-east monsoon). Thus these studies related to the inter-seasonal variation of raindrop size distribution for the south-west and the north-east monsoon over the two cities becomes quite challenging and hence the result from them will be very much helpful for modeling and mapping the urban precipitation pattern. The important conclusion drawn from these studies has been finally portrayed in the Conclusion section of the paper.

2. Data and methodology

The data of raindrop size distribution used in this paper has been taken from two Joss-Waldvogel impact disdrometers placed at the city of Chennai and Mumbai, which are located at the south-eastern and south-western part of Indian sub-continent respectively (Fig. 1). The disdrometer at Chennai is situated at the campus of India Meteorological Department, Meenambakkam, Chennai (13.00°N, 80.18°E) and the disdrometer at Mumbai is also situated at the campus of India Meteorological Department, Santacruz, Mumbai (19.11°N, 72.85°E). The analysis of the DSD over the surface has been done by using the data from these Disdrometers for the year 2019. The rainfall during the month of June–September is considered as the monsoon period or summer monsoon while the rainfall for the month of October-December has been considered as the post-monsoon monsoon months or winter monsoon.

The Disdrometer (Joss and Waldvogel, 1967) is the impact type of Disdrometer that records the number of raindrops hitting 50 cm^2 surface of the sensor thereby enabling the direct estimation of rain integral parameters like rain rate, radar reflectivity and liquid water content. The range of drop diameters that can be measured with this system spans from 0.3 to 5.3 mm and the accuracy of the same is +/− 5% of the measured drop diameter. The outdoor unit of the system senses the raindrops, the diameter of which is further distributed in 20 different channels with a sampling interval of 30 s. The rain-rate R, the radar reflectivity factor Z and Liquid water content (W) are estimated by employing the following standard formula.

$$R = \frac{\Pi}{6} \times \frac{3.6}{10^3} \times \sum_{i=1}^{20} (n_i \times {D_i}^3) \tag{1}$$

$$Z = \left(\frac{1}{F \times t}\right) \sum_{i=1}^{20} \left(\frac{n_i}{v(D_i)} \times D_i^6\right) \tag{2}$$

$$W = \frac{\Pi}{6} \times \frac{1}{F \times t} \times \sum_{i=1}^{20} \left(\frac{n_i}{v(D_i)} \times {D_i}^3\right) \tag{3}$$

where n_i is the number of drops measured in drop size class i during time interval t, D_i is the average diameter of drops in class i, $v(D_i)$ is the fall velocity of drop with diameter D_i, F is the size of sensitive surface of the sensor of disdrometer (0.005m^2) and t is the time interval (30 s). The samples having the rain rate of 1 mm/h and above have been used in the analysis.

The surface temperature and the wind information are obtained from the Automatic Weather Station (AWS), collocated with the Disdrometer at IMD, Chennai.

3. Observational results and discussion

3.1. Inter-seasonal variability of DSD and surface winds over Chennai

In order to find the rainfall distribution with respect to its occurrences (in %) over Chennai during the monsoon and post-monsoon period, the daily rainfall amount (in mm) over the region has been considered and their frequency of occurrences has been plotted in Fig. 2 (a). It is clearly visible from the figure that the rainfall occurrences upto 60 mm/day is dominated for the post-monsoon season while for the monsoon months, the number of days with rainfall occurrences of 70–100 mm/day exceeds the monsoon period. The feature of these daily rainfall occurrences has not been reflected in the mean rain rate as they found to be 9.82 mm/h and 9.28 mm/h during the monsoon and post-monsoon months respectively over Chennai. Correspondingly, the nature of wind direction (in Fig. 2b) during these intra-seasonal phases also shows some interesting results. It is clearly seen from the figure that the monsoon winds over Chennai basically revolves in the region of 260° - 320°, that is the winds originating from the western and north-western direction of Chennai dominates the monsoon period of the city. While for the post-monsoon months, the winds originating from the north-eastern and eastern direction (i.e around 20° - 120°), shows their strong presence over the city. Thus it can be said that the continental and maritime winds dominate the monsoon and post-monsoon season respectively over Chennai.

The microphysical characteristics of rainfall over Chennai during the monsoon and post-monsoon period with respect to the variation of raindrop size distribution (DSD) have been plotted in Fig. 3. No such distinguishing features of DSD are noticed over Chennai during these intra-seasonal phases. Although, a little domination of mid-level drops are observed in the diameter range from 2 to 4 mm during the monsoon period but as a whole the overall features are not so much different to each other with respect to number concentration of smaller, mid-level or larger raindrops.

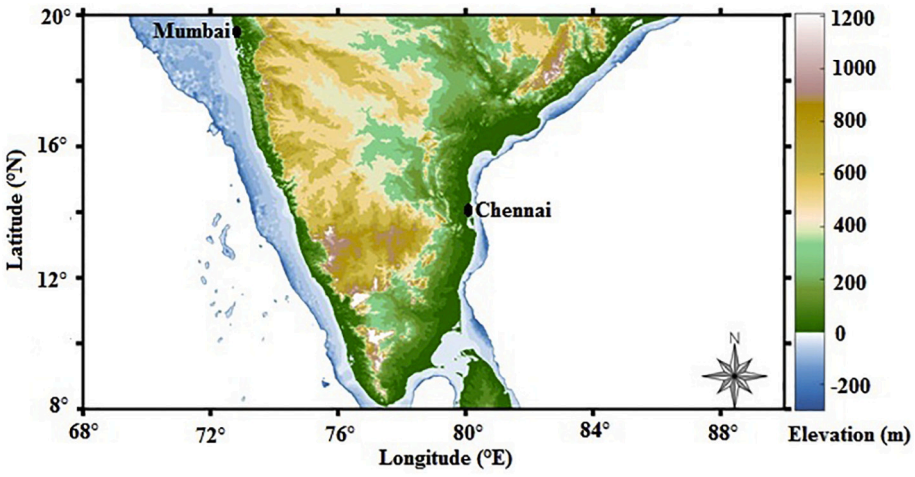

Fig. 1. The topographic map of southern India showing the geographical position of the city of Chennai and Mumbai.

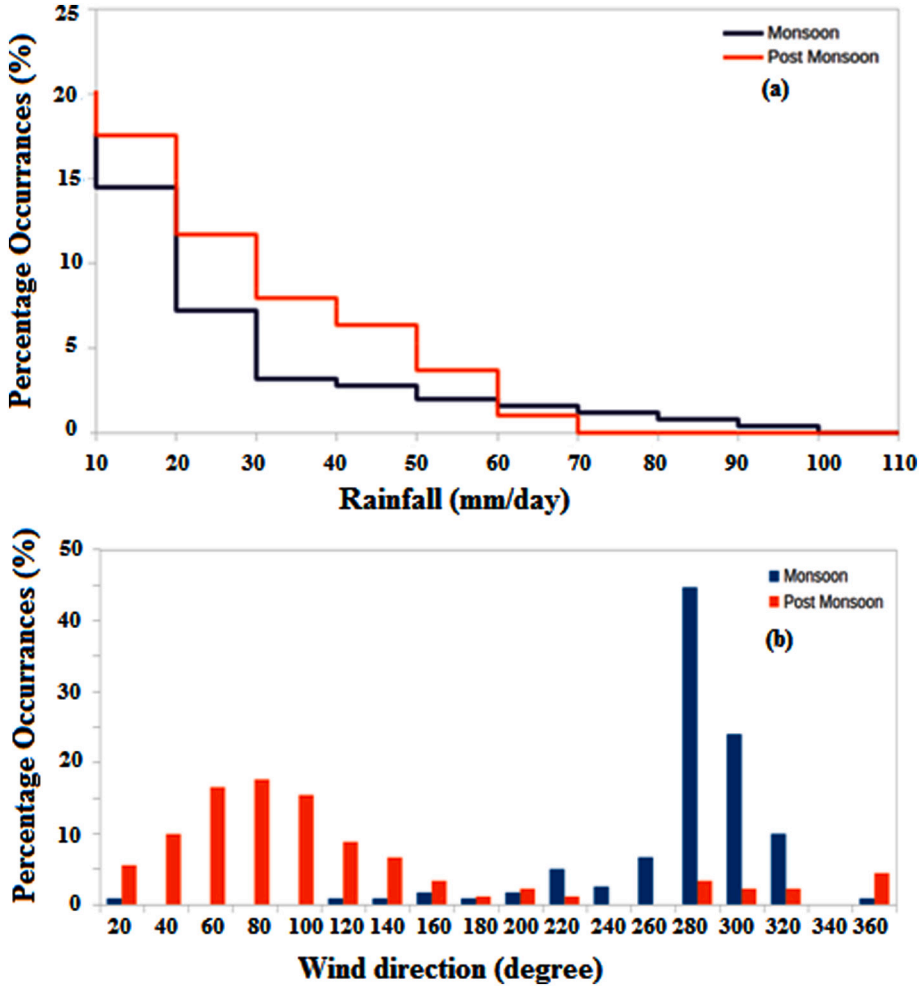

Fig. 2. The distribution of (a) rainfall occurrences (mm/day) and (b) direction of wind (in deg) over the city of Chennai during the monsoon and post-monsoon months. For wind direction, 0° is considered as true north while the angles are considered to progress in the clockwise direction. Thus, 90°, 180° and 270° are considered as east, south and west direction respectively.

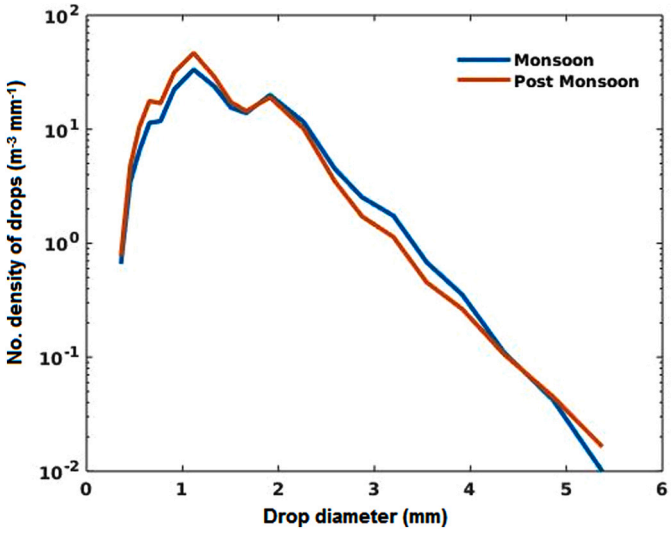

Fig. 3. The variation of raindrop size distribution over the city of Chennai during monsoon and post-monsoon months.

3.2. Diurnal variability over Chennai

Along with the above distribution of rainfall, we move forward by performing an in-depth analysis of the diurnal variation of rainfall and raindrop size distribution over the city for the monsoon and post-monsoon month. Fig. 4(a) and (b) represents the diurnal variation of rainfall occurrences and the corresponding raindrop size distribution for the monsoon period and Fig. 4(c) and (d) represents the same parameters for the post-monsoon period over Chennai. The figure (i.e Fig. 4a) clearly depicts a sharp peak of rainfall occurrences between 14:00–16:00 h during the monsoon period while for the post-monsoon months, although we could not find such distinct peak of rainfall occurrences, but some higher rainfall regions are noticed during 16:00 h (Fig. 4c). At the same time, these higher rainfall regimes for both the monsoon and post monsoon period are associated with the maximum raindrops diameter of 5 mm. It is to be mentioned here that the surface temperature during the monsoon months over Chennai starts increasing from 08:30 h and it becomes highest at 14:30 h (Fig. 5). Thus the air mass in contact with the surface becomes warmer and starts to move in the upward direction in the atmosphere. As the rising air reaches its dew point temperature, water vapour condenses into water droplets or ice. When this pressure becomes more, they try to release it locally which finally falls on the surface as heavy precipitation. As they fall, the water droplets collide with each other and become larger. This is the reason for which we could able to see rainfall peaks accompanying by larger

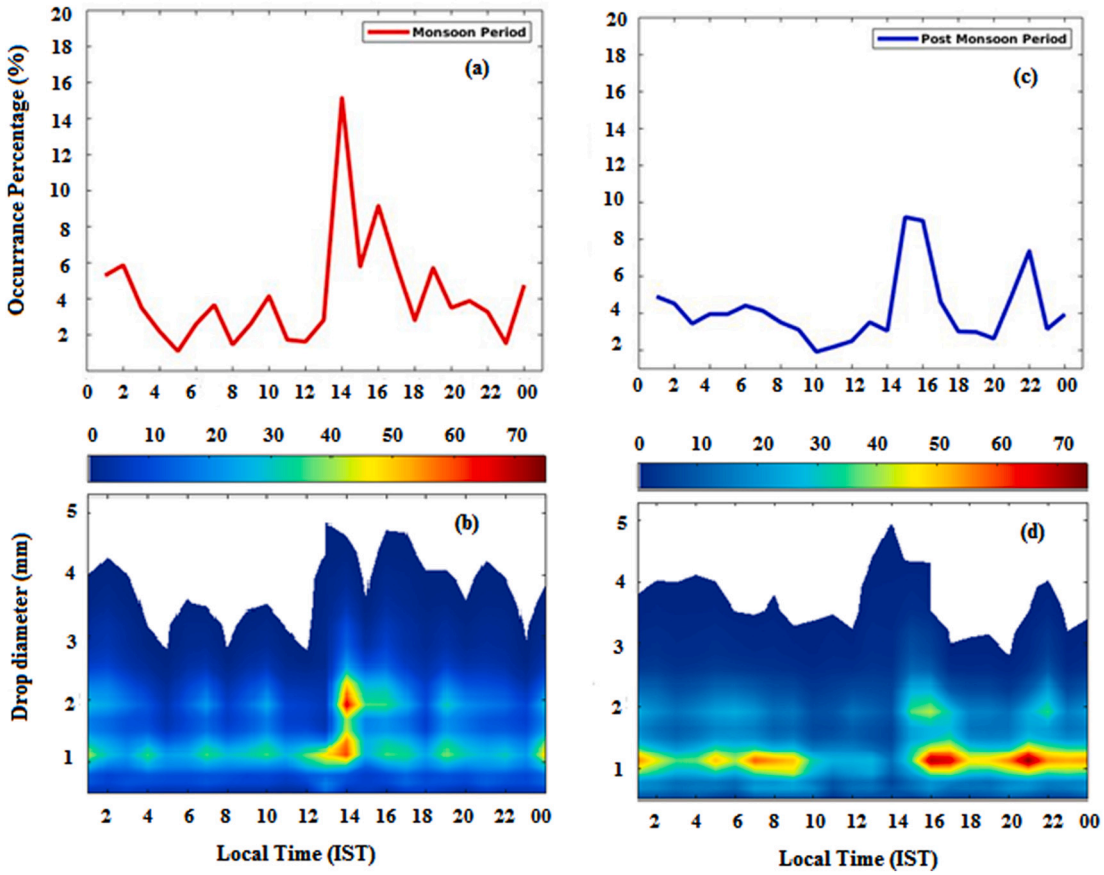

Fig. 4. The diurnal variation of (a) Rainfall and (b) Raindrop size distribution during the monsoon period over the city of Chennai. The similar diurnal variation of (c) Rainfall and (d) Raindrop size distribution during the post-monsoon period over Chennai. The colourbar represents the percentage occurrences of respective raindrops.

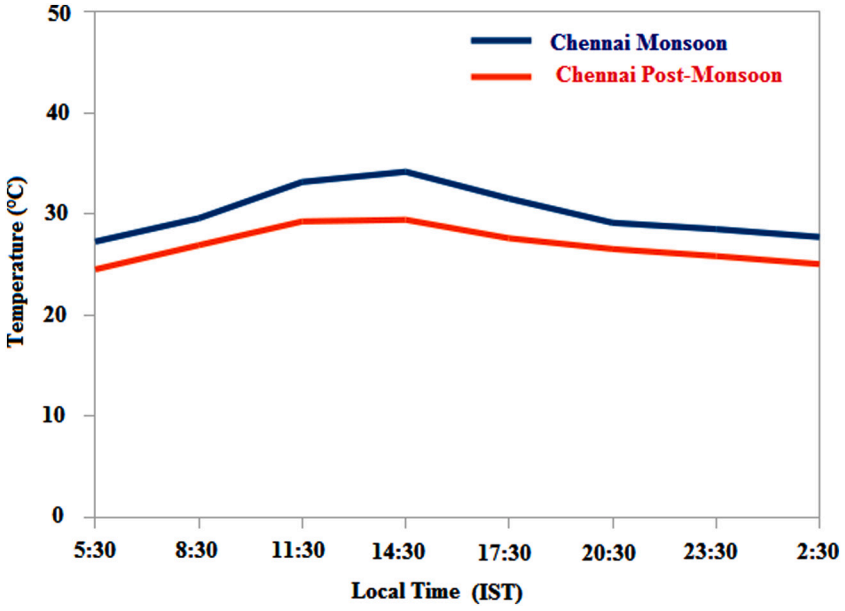

Fig. 5. Diurnal variation of surface temperature during the monsoon and post-monsoon month over the city of Chennai.

raindrops during 13:00–17:00 h for the monsoon period over Chennai. While for the post-monsoon month, the average surface temperature is comparatively low with respect to the monsoon month which signifies that the surface comparatively remains wet in the post-monsoon season. As such the rate of evaporation is also less for which the entire raining process as described above remains low. This is the reason for which we do not get such sharp peaks of rainfall occurrences in the post-monsoon months. The above explanations are also reflected in Fig. 6(a) where the

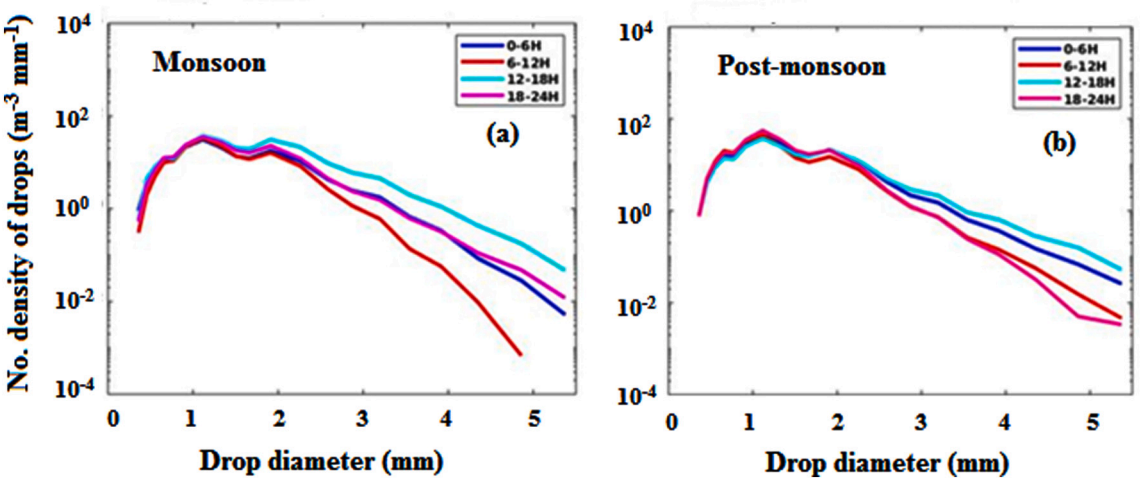

Fig. 6. Quarterly variation of raindrop size distribution for every 6 h during the (a) monsoon and (b) post-monsoon months over the city of Chennai.

quarterly variation of raindrop size distribution has been plotted for the monsoon period over Chennai. The figure clearly portrays that the drops of larger diameter strongly dominates the period from 12:00–18:00 h than any other time of the day which strongly support our findings. While for the post-monsoon month, although similar situations are observed for the variation of DSD (Fig. 6b), but such contrasting difference of the DSD with the other time slots are not visible. Thus it can be said that the degree of atmospheric convection is more during 12:00–16:00 h over Chennai during the monsoon period with respect to post-monsoon months. Along with the diurnal variation, the total rainfall of Chennai during these inter-seasonal phases has been divided into convective, stratiform, weak stratiform and mixed phase on the basis of rain rate, radar reflectivity, mass-weighted mean diameter and maximum drop size as referred by Chang et al. (2009). The occurrences of individual rain classes have been tabled in Table 1. It is clearly seen from the mentioned table that the percentage of convective rainfall with 16.63% is more over Chennai during the monsoon period with respect to the post-monsoon season of 10.92%.

The DSD data of the monsoon and post-monsoon month of Chennai are finally fitted with the three-parameter gamma function from Ulbrich (1983) and the parameters are tabulated in Table 2. The functional form of the gamma distribution is given as.

$$N\ (D) = N_0\ D^{\mu}\ exp.(-\Lambda, D) \tag{4}$$

where D (mm) is the raindrop diameter, $N(D)$ (m^{-3} mm^{-1}) is number of drops per unit volume per unit size interval, N_0 (m^{-3} mm^{-1}) is the intercept parameter, μ is shape parameter and Λ (mm^{-1}) is the slope parameter.

The shape parameter μ is given by

$$\mu = \frac{11G - 8 + \sqrt{G(G+8)}}{2(1-G)} \tag{5}$$

where

Table 1
The variation of convective, stratiform, weak stratiform and mixed phase rainfall over Chennai during the monsoon and post-monsoon season.

Period	Convective (%)	Stratiform (%)	Weak Stratiform (%)	Mixed Phase (%)
Monsoon	16.63	16.02	30.47	36.87
Post-Monsoon	10.92	11.73	37.67	39.67

Table 2
The values of gamma parameters for the monsoon and post-monsoon months over Chennai.

	N_0	Λ	μ
Monsoon	5.7003e+03	3.2276	2.5427
Post-monsoon	6.0892e+03	2.9588	1.5229

$$G = \frac{M_4^3}{M_6 M_3^2} \tag{6}$$

The slope parameter Λ (mm^{-1}) is given by.

$$\Lambda = \frac{(\mu + 4)\mathrm{M}_3}{M_4} \tag{7}$$

where M_3, M_4 and M_6 are the third, fourth and sixth moment of DSD. The shape-slope relation actually indicates the nature of the rain DSD. For a fixed Λ values associated with low μ values indicate presence of large numbers of small drops. For a fixed Λ value, large μ value indicates the concave nature of the DSD due to presence of large number of big drops (Das and Maitra, 2018). The same has been indicated through Table 2 where the signal for the dominance of large raindrops during the monsoon rain in comparison to the post-monsoon months is noticed.

3.3. Inter-seasonal variability over Chennai and Mumbai

Along with Chennai, the paper also tried to explore the inter-seasonal variability of the rainfall microphysics of Chennai with Mumbai – the two urban coastal stations of Indian sub-continent which is situated on the east coast and west coast of India respectively. It has been found from the literatures that in addition to the large-scale dynamic features and urban heating effect, which are generally responsible for the severe rainfall over the cities, the moisture-laden winds from Arabian sea acts as a source of natural aerosols of marine (i.e sea salt) and continental origin (i.e dust aerosol) over the western coast of Indian peninsula thereby impacting the rainfall pattern over the city of Mumbai. In this context, Vinoj et al. (2014) reported that the desert dust aerosol levels over the Arabian Sea, West Asia and Arabian Peninsula are positively correlated with the intensity of the Indian summer monsoon. Correspondingly, by analyzing 11 years multisensor satellite data, Patel et al., 2019, found characteristic signature of dust aerosol-induced modification of thick ice clouds towards strengthened susceptibility of Indian monsoon precipitation. Along with the west coast, some studies related to the characteristics features of aerosol-cloud interaction over east-

coast of Indian peninsula are also available in the literature. By using the aircraft data, Padmakumari et al. (2017) observed higher concentrations of aerosol and cloud condensation nuclei (CCN) over land in comparison to ocean. Correspondingly, over ocean, higher liquid water content (LWC) and lower cloud droplet number concentrations were observed, and droplets reached the threshold of precipitation initiation at lower cloud depths. Thus they highlighted that the convective clouds over land were modified by pollution aerosol with contrasting microphysical properties to those over the ocean. In view of the above discussion related to the impact of aerosols on the precipitation over the eastern and western coast of Indian peninsula, a comparative study of rainfall occurrences during the month of August and October for the year 2019 has been done which thereby represents the monsoon and post-monsoon month respectively for the two stations under consideration. While looking into the percentage of daily rainfall occurrences over the stations, it has been found that the monsoon rainfall over Mumbai dominates the Chennai rainfall (Fig. 7a) while a completely opposite behaviour is seen for the October month when the amount of rainfall in all the steps is more in Chennai with respect to Mumbai (Fig. 7b). Correspondingly, looking into the direction of winds over the cities, it has been found that the westerly winds dominate both the cities during the monsoon time (Fig. 7c). As such, it can be said that the maritime south-westerly, westerly and north-westerly winds engulf the city of Mumbai in the monsoon times while for the city of Chennai, mostly the continental westerly winds with 52% shows their strong presence. Looking into the month of October (Fig. 7d), it has been observed that although the winds are coming from all the directions, but the domination of easterly winds are more for both the cities. Notwithstanding the fact that for Mumbai, the winds are mostly concentrated from the easterly direction (i. from 40° - 160°), but for Chennai, winds originating from the westerly direction are also visible.

3.4. Diurnal variability over Chennai and Mumbai

A comparative study of the diurnal variation of rainfall along with raindrop size distribution during the monsoon and post-monsoon month over the two cities has been portrayed in Fig. 8. The figure reveals that the rainfall occurrences over Mumbai during the month of August do not show any distinct diurnal variation (Fig. 8a). The same pattern could also be found from the variation of raindrop size distribution (Fig. 8b) where the average diameter of raindrops for the entire day remains within 3 mm. While analyzing the rainfall occurrences (Fig. 8c) and raindrop size distribution (Fig. 8d) for the month of October over Mumbai, a different picture is revealed where two sharp peaks of precipitations are noticed at 5:00 h and 12:00 h. Correspondingly, while looking into the dropsize distribution of rainfall, the peak rainfall in 12 noon is reciprocated with the drops of larger diameter. The similar type of analysis had also been performed over Chennai for the month of August and October and the result revealed 3 rainfall peaks in the month of August during 3:30 h, 10:00 h and 17:00 h (Fig. 8e). These rainfall peaks are also accompanied by larger raindrops where the diameter goes upto 4.3 mm (Fig. 8f). At the same time, while looking into the month of October, more rainfall is visible during the early morning hours of 04:00–06:00 h (Fig. 8g). As discussed above, the diurnal variation of surface temperature over the two stations is found to be one of the important factors responsible for these contrasting diurnal features of rainfall pattern. It is already known that the surface temperature of Chennai is always higher than Mumbai in the month of August. At the same time, the continuous downpour over Mumbai during August makes the surface of the city comparatively wet with respect to Chennai. As such the rate of evaporation and therefore the tendency of upward movement of warm air parcels over Chennai is more with respect to Mumbai during monsoon period. This builds up the higher probability of convective environment in Chennai which ultimately results for these scattered regions of higher rainfall occurrences along with larger drops in Chennai with respect to Mumbai in the monsoon month. Although the afternoon peak of rainfall can be addressed with the above scientific explanations, but there exists several thoughts related to the morning rainfall peaks during the months of August and October over Chennai and Mumbai respectively. Some scholars suggest that precipitation peaks occurring at night result from stratiform precipitation which is enhanced by instability caused by radiative cooling near the cloud top at night time (Lin et al., 2000) while others believe that the accumulation of the water vapour in the lower layer of atmosphere promotes the nocturnal convection significantly (Nesbitt and Zipser, 2003).

3.5. D_0-W relationship between Chennai and Mumbai

As both of cities of Mumbai and Chennai are basically the coastal stations of Arabian Sea and Bay of Bengal respectively, hence it was essential to study the impact of maritime and continental rainfall on those two cities. As such a classification of the two has been done by

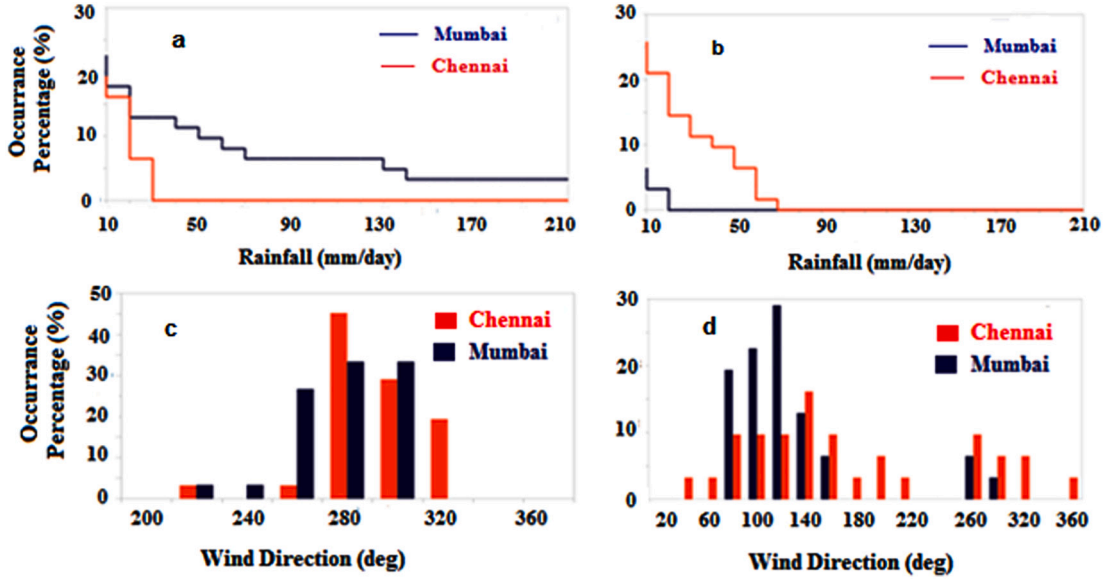

Fig. 7. The distribution of (a) rainfall occurrences and (cc) wind direction during the month of August over the city of Chennai and Mumbai. The similar distribution of (bb) rainfall occurrences and (d) wind direction during the month of October over the city of Chennai and Mumbai.

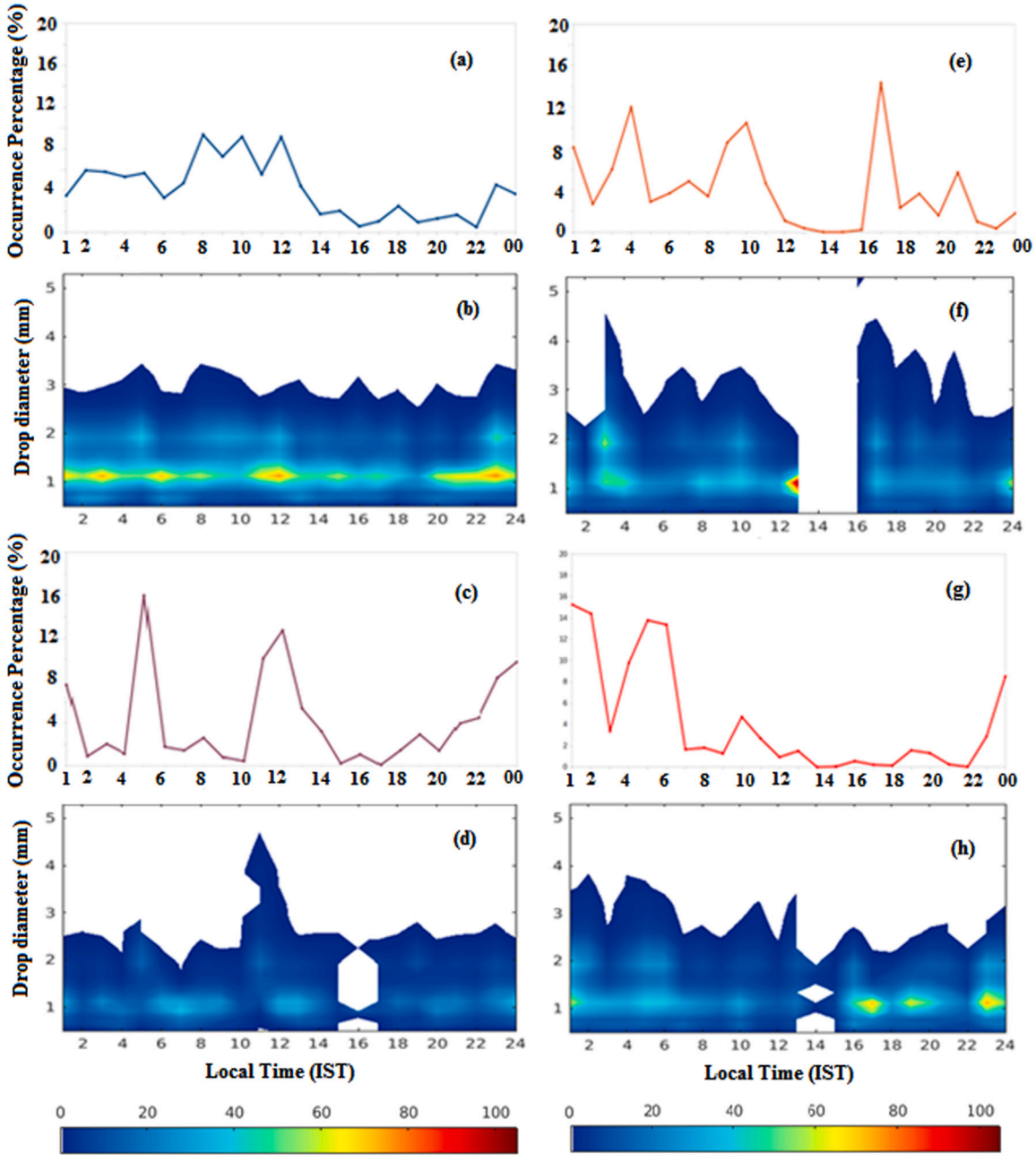

Fig. 8. Diurnal variation of (a) rainfall occurrences and (b) raindrop size distribution for the month of August-2019 over Mumbai. The similar diurnal variation of (c) rainfall occurrences and (d) raindrop size distribution for the month of October-2019 over Mumbai. The Diurnal variation of (e) rainfall occurrences and (f) raindrop size distribution for the month of August-2019 over Chennai. The similar diurnal variation of (g) rainfall occurrences and (h) raindrop size distribution for the month of October-2019 over Chennai. The colourbar represents the percentage occurrences of respective raindrops.

using the available *Z-R* relationship which were derived from the surface-based raindrop size distribution measurements and can be related to a relative scale of estimated continentality-maritimity of the clouds. The values of coefficient *A* and exponent *b* listed in Table 3 are obtained from the Z-R relationship whereas the values of raindrop size distribution parameters N_0 and μ are calculated from A and b using the equation portrayed in Rosenfeld and Ulbrich, 2003.

$$N_0 = \left\{ \frac{A\left[33.31\Gamma\left(\frac{2.33}{b-1}\right)\right]^b}{10^6\Gamma\left(\frac{2.33b}{b-1}\right)} \right\}^{1/(1-b)} \quad (8)$$

Table 3
Values of Median volume diameter (D_0) and Liquid water content (W_0) as derived from *A* and *b* for a fixed rain rate of 30 mm/h.

Class	*A*	*b*	D_0 (30) [cm]	W_0 (30) [g/m^3]
Marshall Island maritime wind (Stout and Mueller, 1968)	126.00	1.47	0.1340	1.7610
Mumbai (August – 2019)	186.20	1.40	0.1580	1.5847
Mumbai (October – 2019)	257.03	1.45	0.1545	1.6029
Chennai (August – 2019)	269.15	1.38	0.1982	1.3632
Chennai (October – 2019)	281.83	1.33	0.2433	1.1920
Swiss Locarno Thunderstorm (Joss and Waldvogel, 1970)	830.00	1.50	0.3080	1.0070

$$\mu = \frac{7 - 4.67b}{b - 1} \tag{9}$$

These values are further used to derive median volume diameter (D_0) and liquid water concentration (W) for a fixed rain rate of 30 mm/h using the equations as follows.

$$D_0 = \varepsilon R^{\delta}; \varepsilon = \frac{3.67 + \mu}{[33.31 N_0 \Gamma(4.67 + 1)]^{1/(4.67+\mu)}}; \delta = \frac{1}{4.67 + \mu} \tag{10}$$

$$W = \zeta R^{\kappa}; \zeta = \frac{\pi \Gamma(4 + \mu) N_0^{0.67/(4.67+\mu)}}{6[33.31 \Gamma(4.67 + \mu)]^{(4+\mu)/(4.67+\mu)}}; \kappa = \frac{4 + \mu}{4.67 + \mu} \tag{11}$$

where R denotes the rain rate in mm/h. The total rainfall is segregated into 4 categories and the corresponding values of D_0 and W derived from above are tabulated in Table 3 for the fixed rain rate of 30 mm/h. In order to find the characteristic features of continental and maritime type of clouds, the similar types of values as obtained from the various parts of the world have been collected from literatures (Rosenfeld and Ulbrich, 2003) and also tabulated in Table 3. A relationship between the D_0-W has been portrayed in Fig. 9 from which the corresponding continental-maritime separation has been performed as per Rosenfeld and Ulbrich, 2003. It is to be hereby noted that the method employed in this work finds theoretical $D_0 - W$ relationship that are used for classifying the type of rainfall even though they may not be accurate representation of the actual empirical relations. Nevertheless, Atlas (1964) has shown that $D_0 - R$ relationship found from Z-R relationship that he investigated are in good agreement with those found directly from empirical drop-size spectra. Thus from Fig. 9 it has been found that the rainfall for both the monsoon and post-monsoon season over Mumbai are maritime in nature while the rainfall in Chennai in the month of August fall in the intermediate category as it bears the properties of both maritime and continental phase. While the rainfall in the month of October for Chennai stands at the junction of the ending of intermediate phase and starting of continental phase.

3.6. Variation of rain rate and DSD for fixed radar reflectivity

The same R-Z relationship is further applied in Fig. 10 where the corresponding rain rate has been achieved for a fixed radar reflectivity of 30 dBZ and 40 dBZ. It is quite interesting to note that rain rate increases for increase maritimity of clouds. Thus for Fig. 10a, which represents the rain rate for the fixed radar reflectivity of 30 dBZ, it is seen that the rainfall for the month of August in Mumbai possess strong maritime behaviour while the October month of Chennai has the least maritime effect compared to the other three. Correspondingly, while looking into the rain rate pattern for the fixed radar reflectivity of 40 dBZ (Fig. 10b), interestingly the extreme maritimity is observed for the rainfall in the month of October over Chennai which are followed by the rainfall for the month of August in Mumbai and Chennai followed by rainfall in October over Mumbai respectively. This contrasting behaviour of the degree of maritimity of the post-monsoon rainfall over Chennai for 30 dBZ and 40 dBZ has been further studied with respect to the variation of raindrop size distribution for those fixed radar reflectivity and portrayed in Fig. 11. It is quite visible from the month of August that the raindrops in the diameter range of 2.5 mm dominates the rainfall over Chennai (Fig. 11a) while for the month of October, although the domination is slightly more over Chennai for the raindrops in the diameter range of 1–3 mm, but as a whole no such wide differences in the variation of drop diameter are visible in the lower and higher diameter range for the post-monsoon rainfall of two cities (Fig. 11b). Thus in order to find in details the variation of raindrop size distribution for a fixed radar reflectivity, the similar type of analysis has been performed for radar reflectivity of 40 dBZ and 30 dBZ. It is clearly seen from the figure that at the fixed radar reflectivity of 30 dBZ, raindrops of diameter 2–3 mm shows a strong domination for the Chennai rainfall with respect to the Mumbai for both the monsoon (Fig. 11c) and post-monsoon month (Fig. 11d). Correspondingly, for the radar reflectivity of 40 dBZ, some contrasting behaviour is noticed where the raindrops of diameter 2.5–5 mm for the Chennai rainfall dominates the Mumbai rainfall during the monsoon month (Fig. 11e) while for the post-monsoon period, the situation reverses as raindrops in the same diameter range shows its strong domination for the Mumbai rainfall (Fig. 11f). It is already revealed through Fig. 9 that median volume diameter of the raindrops increases on the increasing continentality of the rainfall, hence the above observations related to the variation of DSD over Chennai during monsoon months supports the findings in Fig. 11. While, in case of Mumbai during the month of October, the city receives rainfall from both the south-west monsoon, which is maritime in nature and north-east monsoon, which is a continental type. Thus in case of 30 dBZ, we observe the maritime nature of the Mumbai rainfall but in case of 40 dBZ, the continental trend over the Mumbai rainfall is strongly visible (Fig. 10a and b respectively). This is the reason for which we

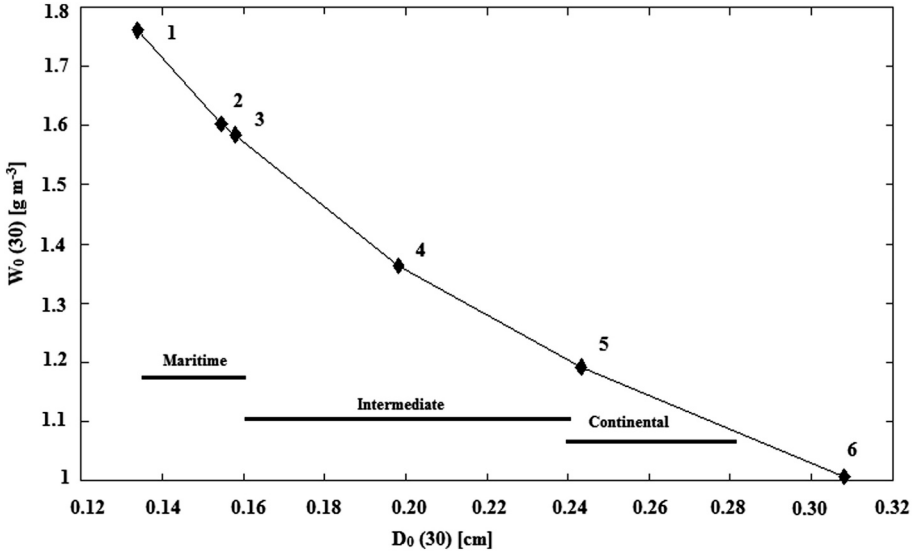

Fig. 9. The relationship between the Liquid water content W and median volume diameter D_0 for the fixed rain rate of 30 mm/h in the continental and maritime regimes. The rainfall regimes against the particular number has been listed as follows – (1) Marshal island maritime winds (2) Mumbai rainfall during October (3) Mumbai rainfall during August (4) Chennai rainfall during August (5) Chennai rainfall during October (6) Swiss Locarno Thunderstorm.

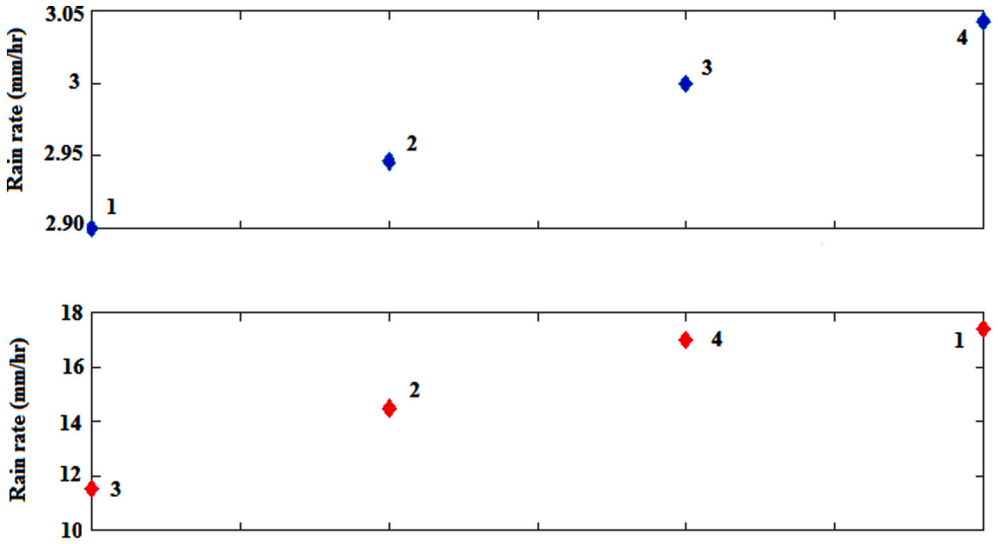

Fig. 10. The *Z*-R relations for rainfall from maritime and continental clouds. The rain intensities (mm/h) for (a) 30 dBZ and (b) 40 dBZ are plotted in the figure. The numbers in the figure indicate the following events – (1) Chennai rainfall during October (2) Chennai rainfall during August (3) Mumbai rainfall during October and (4) Mumbai rainfall during August. A systemic increase of rain rate for a given radar reflectivity is noticed for the transition from continental to maritime clouds.

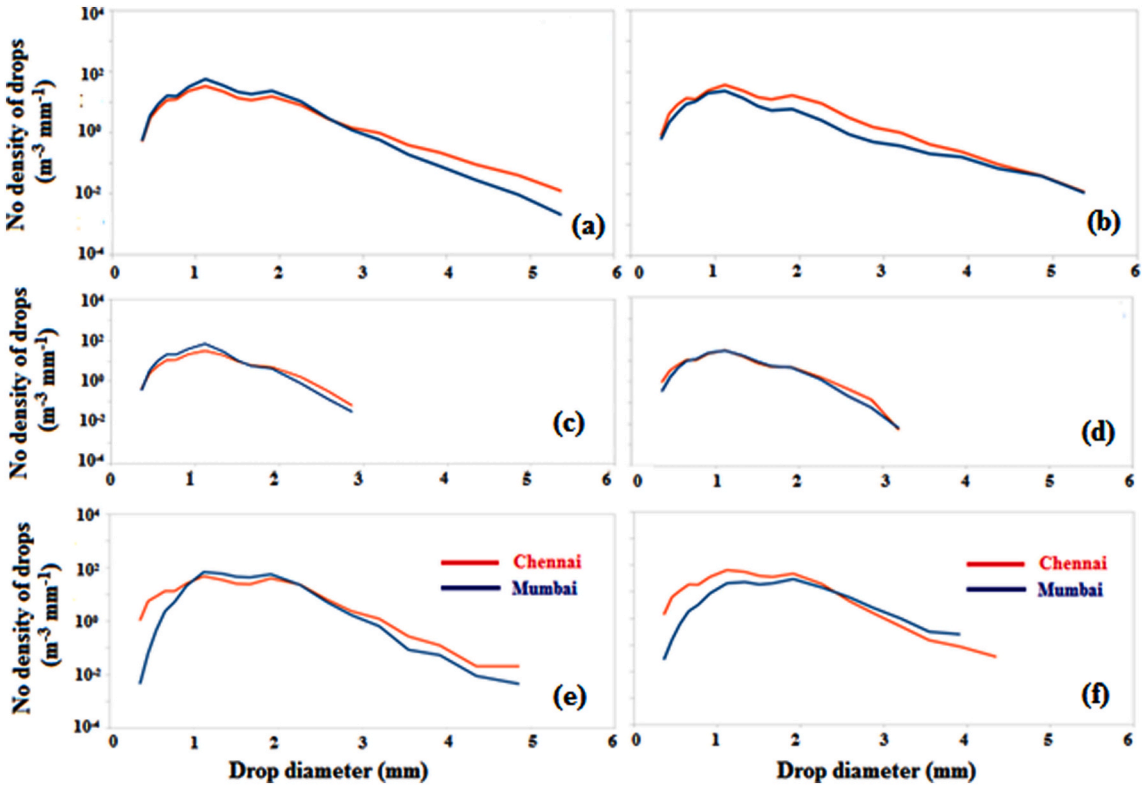

Fig. 11. The variation of raindrop size distribution over Chennai and Mumbai for the month of (a) August and (b) October respectively. The variation of raindrop size distribution over Chennai and Mumbai for fixed radar reflectivity of 30 dBZ for the month of (c) August and (d) October respectively. The variation of raindrop size distribution over Chennai and Mumbai for fixed radar reflectivity of 40 dBZ for the month of (e) August and (f) October respectively.

observe the contrasting variation of DSD over Mumbai and Chennai during the month of August and October.

3.7. Rainfall integrated parameters for fixed rain rate classes

The relationship between the rainfall parameters during the monsoon(i.e August) and post-monsoon (i.e October) month over the two cities have been finally portrayed through Fig. 12. The total rainfall over the cities has been divided into 7 different categories (same as Rao et al., 2009) with respect to rain intensity regimes namely, 1 ≤Rain rate (mm/h) < 2 (Class-1), 2 ≤Rain rate(mm/h) <4 (Class-2), 4 ≤Rain rate (mm/h) < 8 (Class-3), 8 ≤Rain rate (mm/h) < 16 (Class-4), 16 ≤Rain rate(mm/h) < 32 (Class-5), 32 ≤Rain rate(mm/h) < 64 (Class 6) and 64 ≤ Rain rate (mm/h) (Class-7). It is clearly visible that the average rainfall intensity is slightly more in Chennai from Class-5 onwards for both the monsoon (Fig. 12a) and post-monsoon (Fig. 12b) period. While

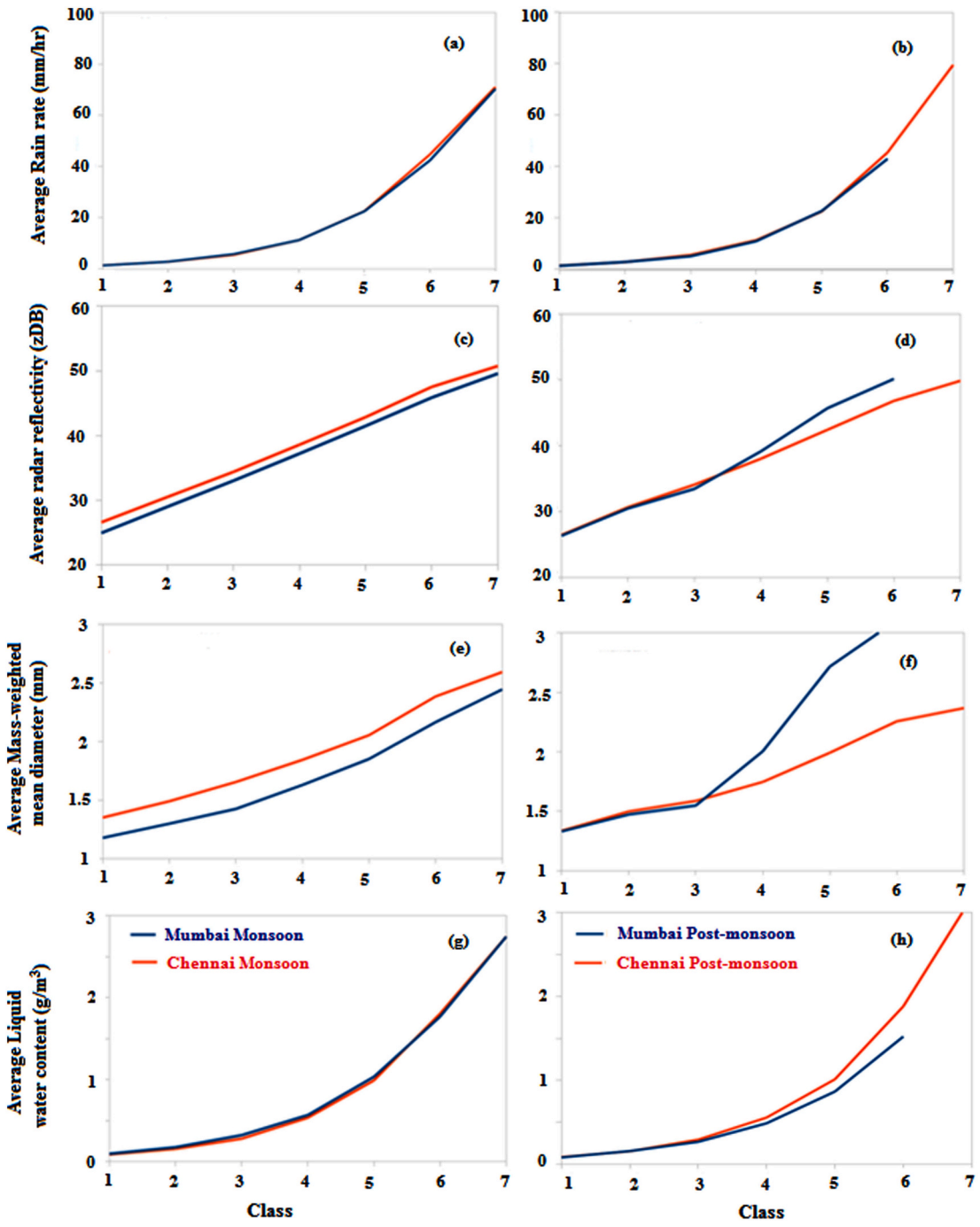

Fig. 12. Comparative study of the variation of rainfall integrated parameter during the monsoon (August) and post-monsoon month (October) over Chennai and Mumbai for 7 rain rate regimes as portrayed in the manuscript. The variation of average rain rate (mm/h) during (a) Monsoon and (b) Post-monsoon month. The variation of average radar reflectivity (dBZ) during the (c) Monsoon and (d) Post-monsoon month. The variation of average mass-weighted mean diameter (mm) during the (e) Monsoon and (f) Post-monsoon month. The variation of average liquid water content (gm/m^3) during the (e) Monsoon and (f) Post-monsoon month.

looking into the radar reflectivity factor it has been found that the average radar reflectivity remains high in respect of all the classes for the monsoon period of Chennai (Fig. 12c) while for the post-monsoon period, the situation starts to toggle from Class – 4 onwards where domination of higher reflectivity is noticed in case of Mumbai for the higher rain rate regimes (Fig. 12d). The same situation is reflected for the variation of median volume diameter where the strong domination of larger drop diameter is noticed for all the classes in case for the monsoon month over Chennai (Fig. 12e). While for the post-monsoon period, a strong domination of larger drops is visible from Class-3 onwards in case of the Mumbai rainfall (Fig. 12f). It is already discussed in the previous section of this paper that mass-weighted mean diameter of the raindrops is more for the rainfall originating from the continental clouds with respect to the maritime ones. Thus during the south-west monsoon period, the rainfall over Chennai has the more continental effect than the maritime ones as the maritime clouds from the west travels a long distance through the Indian landmass from western to eastern direction to provide rainfall in the east-coast of Indian peninsula. The same situation also holds true for the post-monsoon rainfall over Mumbai for higher rain rate regimes. Generally, during the month of October, Mumbai receives rain from both from the withdrawal phase of south-west monsoon and onset phase of north-east monsoon. The north-

east monsoon after travelling the land surface from eastern to western direction of Indian Peninsula ushers heavy rainfall over Mumbai city. This propagation of clouds through the land surface provides the continental impact in the characteristic features of rainfall that ultimately escalates the average value of mass-weighted diameter and thereby radar reflectivity factor for the post-monsoon rainfall over Mumbai with respect to Chennai. Finally, in case of the liquid water content (LWC), the monsoon rainfall does not display any strong variations as the values increases uniformly for both the cities (Fig. 12g). As for example, the lowest and highest average values of LWC in Class-1 and Class-7 are 0.093 g/m^3 and 2.742 g/m^3 for Mumbai respectively while the same values for Chennai reads 0.085 g/m^3 and 2.743 g/m^3 respectively. Correspondingly, the post-monsoon month shows a slight different behaviour where the domination of LWC from Class-4 onwards is strongly visible for Chennai rainfall over the Mumbai ones (Fig. 12h). The effect of continental and maritime atmosphere prevailing over these stations during various stages of the inter-seasonal phases has sufficiently impacted on the behaviour of the microphysical properties of rainfall over the two stations correspondingly.

4. Summary and conclusion

The present paper tried to highlight the inter-seasonal variation of raindrop size distribution over Mumbai and Chennai - the two urban-coastal station of Indian sub-continent which differs contrastingly with respect to their rainfall occurrences. The south-west monsoon (also known as summer monsoon) from Arabian sea and north-east monsoon (also known as winter monsoon) from Bay of Bengal dominates the cities of Mumbai and Chennai during the monsoon and post-monsoon months respectively. We started the paper by analyzing the microphysical properties of rainfall over Chennai, which lies on the south-eastern part of Indian sub-continent and correspondingly act as a windward side for the north-east monsoon and leeward side for the south-west monsoon due to the presence of Eastern ghat mountain range which runs parallel to the east-coast of peninsular India. Although, the study revealed a mild domination of larger raindrops (of diameter 5 mm and above) for the post-monsoon period with respect to the monsoon months, but on the whole the region experiences higher concentration of mid-level drops (2–4 mm) during the monsoon period. The same is also reflected in the amount of convective and stratiform rainfall as the amount of convective rainfall exceeds in the monsoon period with respect to the post-monsoon months. While looking into the diurnal variation, a sharp peak of rainfall occurrences along with larger drops is visible during the monsoon period. This is basically due to the increase of surface heating during the monsoon period around 12:00–14:00 h which through rapid evaporation generates sufficient water vapour in the upper atmosphere that finally end up with heavy precipitation for some pocket of time. While in the case of post-monsoon period, the surface temperature is comparatively less for which the rate of evaporation is low and as a result, we do not get such pointed rainfall peaks in the post-monsoon period over Chennai.

Along with Chennai, the paper also tried to highlight the microphysical properties of precipitation over Mumbai and as such, a comparative study has been done between the two cities. As both the cities lies across the sea coast, so the continental and maritime clouds do have a strong impact on the seasonality of monsoon. The study reveals that during the monsoon month, drops of larger diameter dominate the rainfall over Chennai with respect to Mumbai for all rain rate regimes. Correspondingly, for the post-monsoon month, comparatively larger drops are visible for low rain rate regimes upto 10 mm/h in case of Chennai rainfall but the situation starts to reverse for higher rain rates, where strong existence of bigger drops are visible for the Mumbai rainfall. The situation is also seen in case of radar reflectivity where the higher reflectivity is noticed for the higher rain rate regimes of 16 mm/h and above in case of the post-monsoon rainfall of Mumbai. This is due to the fact that the monsoon rainfall over Mumbai is purely maritime in nature due to south-west monsoon from Arabian Sea hitting the city from the windward side of the Western ghat. While for the post-monsoon rain, although Mumbai receives the rainfall from the Arabian Sea branch of monsoon, but the chunk of severe rainfall happens to be continental in nature as it comes from the south-eastern direction of the city as a part of north-east monsoon. The similar case is also true for Chennai where both the maritime and continental impact over the city is visible during the monsoon months as the city receives rainfall from both the Arabian sea and Bay of Bengal branch of Indian summer monsoon. These continental-maritime effects in combination with the surface temperature also had a strong impact on the diurnal variability of rainfall occurrence. Observation reveals the occurrences of sharp rainfall peaks in the August and October month over Chennai and Mumbai respectively which ultimately highlights the fact that the rainfall originating from the continental clouds do possess a strong diurnal variations.

Thus on the whole it can be concluded that this high-spatiotemporal-resolution dataset of two heavily populated cities has provided a new, comprehensive insight regarding the microphysical characteristics of precipitation over the two urban-coastal stations of India which acts as a reference point for the precipitation pattern of south-west and north-east monsoon rainfall over Indian sub-continent.

Declaration of Competing Interest

None.

Acknowledgement

Indian Institute of Tropical Meteorology, Pune is funded by the Ministry of Earth Sciences, Government of India. We thank the Director, IITM for his continuous support and encouragement. We would like to thank K.S. Hosalikar and Jaan Mohmmad from India Meteorological Department (IMD), Mumbai and S.Balachandran and N.Meenatchi Nathan from IMD, Chennai for providing full support for operating Disdrometer in their respective office campus. We also like to thank Anjit Anjan of IMD, Pune for providing the AWS data. Finally, we sincerely thank the Editor, Associate Editor and other two anonymous reviewers for their critical and constructive comments related to the improvement of the manuscript. The disdrometer data, which are archived at IITM can be available with the Corresponding author (kaustav@tropmet.res.in) for any scientific collaborations.

References

Altaratz, O., Koren, I., Remer, L.A., Hirsch, E., 2014. Review: cloud invigoration by aerosols-coupling between microphysics and dynamics. Atmos. Res. 140, 38–60.

Atlas, D., 1964. Advances in radar meteorology. Adv. Geophys. 10, 317–478.

Atlas, D., Ulbrich, C.W., Marks Jr., F.D., Amitai, E., Williams, C.R., 1999. Systematic variation of drop size and radar-rainfall relations. J. Geophys. Res. 104, 6155–6169.

Baker, R.D., Lynn, B.H., Boone, A., Tao, W.K., Simpson, J., 2001. The influence of soil moisture, coast curvature and land-breeze circulations on sea-breeze-initiated precipitation. J. Hydrometeorol. 2, 193–211.

Bergemann, M., Jakob, C., 2016. How important is tropospheric humidity for coastal rainfall in the tropics? Geophys. Res. Lett. 43, 5860–5868.

Bringi, V., Chandrasekar, V., Hubbert, J., Gorgucci, E., Randeu, W.L., Schoenhuber, M., 2003. Raindrop size distribution in different climatic regimes from disdrometer and dual-polarized radar analysis. J. Atmos. Sci. 60 (2), 354–365. https://doi.org/10.1175/1520-0469(2003)060%3C0354:RSDIDC%3E2.0.CO;2.

Chakravarty, K., Raj, P.E., 2013. Raindrop size distributions and their association with characteristics of clouds and precipitation during monsoon and post-monsoon periods over a tropical Indian station. Atmos. Res. 124, 181–189. https://doi.org/10.1016/j.atmosres.2013.01.005.

Chakravarty, K., Raj, P.E., Bhattacharya, A., Maitra, A., 2013. Microphysical characteristics of clouds and precipitation during pre-monsoon and monsoon period over a tropical Indian station. J. Atmos. Solar-Terrestrial Phys. 94, 28–33. https://doi.org/10.1016/j.jastp.2012.12.016.

Chang, W.Y., Wang, T.C.C., Lin, P.L., 2009. Characteristics of the raindrop size distribution and drop shape relation in typhoon systems in the Western Pacific from the 2D video disdrometer and NCU C-band polarimetric radar. J. Atmos. Ocean. Technol. 26, 1973–1993. https://doi.org/10.1175/2009JTECHA1236.1.

Chen, X.C., Zhao, K., Xue, M., Zhou, B.W., Huang, X.X., Xu, W.X., 2015. Radar-observed diurnal cycle and propagation of convection over the Pearl River Delta during Mei-Yu season. J. Geophys. Res. Atmos. 120, 12557–12575.
Das, S., Chatterjee, C., 2018. Rain characterization based on maritime and continental origin at a tropical location. J. Atmos. Solar-Terrestrial Phys. 173, 109–118.
Das, S., Maitra, A., 2018. Characterization of tropical precipitation using drop size distribution and rain rate-radar reflectivity relation. Theor. Appl. Climatol. 132, 275–286. https://doi.org/10.1007/s00704-017-2073-1.
Das, S.K., Konwar, M., Chakravarty, K., Deshpande, S.M., 2017. Raindrop size distribution of different cloud types over the Western Ghats using simultaneous measurements from micro-rain radar and disdrometer. Atmos. Res. 186, 72–82. https://doi.org/10.1016/j.atmosres.2016.11.003.
Dimri, A.P., Yasunari, T., Kotlia, B.S., Mohanty, U.C., Sikka, D.R., 2016. Indian winter monsoon: present and past. Earth-Sci. Rev. 163, 297–322. https://doi.org/10.1016/j.earscirev.2016.10.008.
Feingold, G., Cotton, W.R., Kreidenweis, S.M., Davis, J.T., 1999. The impact of giant cloud condensation nuclei on drizzle formation in stratocumulus: Implications for cloud radiative properties. J. Atmos. Sci. 56, 4100–4117.
Geotis, S.G., Houze, R.A., 1985. Rain amounts near and over North Borneo during winter Monex. Mon. Weather Rev. 113, 1824–1828. https://doi.org/10.1175/1520-0493(1985)113<1824:RANAON>2.0.CO;2.
Harikumar, R., Sampath, S., Sasi Kumar, V., 2009. An empirical model for the variation of rain drop size distribution with rain rate at a few locations in southern India. Adv. Space Res. 43, 837–844.
Holland, G.J., Keenan, T.D., 1980. Diurnal variations of convection over the "Maritime Continent". Mon. Weather Rev. 108 (2), 223–225.
Hou, A.Y., Skofronick-Jackson, G., Kummerow, C.D., Shepherd, J.M., 2008. Global precipitation measurement. In: Michaelides, S. (Ed.), Precipitation: Advances in Measurement, Estimation and Prediction. Springer, New York, pp. 131–169. https://doi.org/10.1007/978-3-540-77655-0_6.
Iguchi, T., Kozu, T., Meneghini, R., Awaka, J., Okamoto, K., 2000. Rain-profiling algorithm for the TRMM precipitation radar. J. Appl. Meteorol. 39 (12), 2038–2052. https://doi.org/10.1175/1520-0450(2001)040%3C2038:RPAFTT%3E2.0.CO;2.
Iwasaki, H., Nii, T., Sato, T., Kimura, F., Nakagawa, K., Kaihotsu, I., Koike, T., 2008. Diurnal variation of convective activity and precipitable water around Ulaanbaator, Mongolia, and the impact of soil moisture on convective activity during nighttime. Mon. Weather Rev. 136, 1401–1415. https://doi.org/10.1175/2007MWR2062.1.
Jameson, A.R., Larsen, M.L., Kostinski, A.B., 2015. Disdrometer network observations of finescale spatial–temporal clustering in rain. J. Atmos. Sci. 72 (4), 1648–1666. https://doi.org/10.1175/JAS-D-14-0136.1.
Jash, D., Resmi, E.A., Unnikrishnan, C.K., Sumesh, R.K., Sreekanth, T.S., Nita, S., Ramachandran, K.K., 2019. Variation in rain drop size distribution and rain integral parameters during southwest monsoon over a tropical station: an inter-comparison of disdrometer and Micro rain Radar. Atmos. Res. 217, 24–36.
Jirak, I.L., Cotton, W.R., 2006. Effect of air pollution on precipitation along the Front Range of the Rocky Mountains. J. Appl. Meteorol. Climatol. 45, 236–245.
Joss, J, Waldvogel, A, 1967. A spectrograph for raindrops with automatic interpretation. Geofis. Pura Appl. 68, 240–246.
Joss, J., Waldvogel, A., 1970. A Method to Improve the Accuracy of Radar Measured Amounts of Precipitation. Preprints, 14th Radar Meteorology Conf. Amer. Meteor. Soc, Tucson, AZ, pp. 237–238.
Jung, S.A., Lee, D.-I., Jou, B.J.-D., Uyeda, H., 2012. Microphysical properties of maritime squall line observed on June 2, 2008 in Taiwan. J. Meteorol. Soc. Jpn. 90 (5), 833–850. https://doi.org/10.2151/jmsj.2012-516.
Kousky, V.E., 1980. Diurnal rainfall variation in Northeast Brazil. Mon. Weather Rev. 108 (4), 488–498. https://doi.org/10.1175/1520-0493(1980)108<0488:DRVINB>2.0.CO;2.
Kozu, T., Iguchi, T., Kubota, T., Yoshida, N., Seto, S., Kwiatkowski, J., Takayabu, Y.N., 2009a. Feasibility of raindrop size distribution parameter estimation with TRMM precipitation radar observations of shallow convection with a rain cell model. J. Meteorol. Soc. Jpn. 87A, 53–66. https://doi.org/10.2151/jmsj.87A.53.
Kozu, T., Shimomai, T., Kashiwagi, N., 2009b. Raindrop size distribution modeling from a statistical rain parameter relation and its application to the TRMM precipitation radar rain retrieval algorithm. J. Appl. Meteorol. Climatol. 48 (4), 716–724. https://doi.org/10.1175/2008JAMC1998.1.
Kripalani, R.H., Kumar, P., 2004. Northeast monsoon rainfall variability over south peninsular India Vis-à-Vis the Indian Ocean dipole mode. Int. J. Climatol. 24, 1267–1282. https://doi.org/10.1002/joc.1071.
Kumar, P., Kumar, K.R., Rajeevan, M., Sahai, A.K., 2007. On the recent strengthening of the relationship between ENSO and northeast monsoon rainfall over South Asia. Clim. Dyn. 28, 649–660. https://doi.org/10.1007/s00382-006-0210-0.
Lavanya, S., Kirankumar, N.V.P., Aneesh, S., Subrahmanyama, K.V., Sijikumar, S., 2019. Seasonal variation of raindrop size distribution over a coastal station Thumba: a quantitative analysis. Atmos. Res. 229, 86–99.
Liao, L., Meneghini, R., Tokay, A., 2014. Uncertainties of GPM DPR rain estimates caused by DSD parameterizations. J. Appl. Meteorol. Climatol. 53 (11), 2524–2537. https://doi.org/10.1175/JAMC-D-14-0003.1.
Lin, X., Randall, D.A., Fowler, L.D., 2000. Diurnal variability of the hydrologic cycle and radiative fluxes: Comparisons between observations and a GCM. J. Climatol. 13, 4159–4179.
Maki, M., Keenan, T.D., Sasaki, Y., Nakamura, K., 2001. Characteristics of the raindrop size distribution in tropical continental squall lines observed in Darwin, Australia. J. Appl. Meteorol. 40 (8), 1393–1412 (doi:10.1175/1520-0450(2001)040<1393:COTRSD>2.0.CO;2).
Marzano, F.S., Cimini, D., Montopoli, M., 2010. Investigating precipitation microphysics using ground-based microwave remote sensors and disdrometer data. Atmos. Res. 97 (4), 583–600. https://doi.org/10.1016/j.atmosres.2010.03.019.
Marzuki, M., Hashiguchi, H., Yamamoto, M.K., Mori, S., Yamanaka, M.D., 2013. Regional variability of raindrop size distribution over Indonesia. Ann. Geophys. 31, 1941–1948.
Moumouni, S., Gosset, M., Houngninou, E., 2008. Main features of rain drop size distributions observed in Benin, West Africa, with optical disdrometers. Geophys. Res. Lett. 35 (23), L23807. https://doi.org/10.1029/2008GL035755.
Nakamura, K., Iguchi, T., 2007. Dual-wavelength radar algorithm. In: Levizanni, V., Bauer, P., Turk, F.J. (Eds.), Measuring Precipitation from Space. Springer, New York, pp. 225–234. https://doi.org/10.1007/978-1-4020-5835-6_18.
Nesbitt, S.W., Zipser, E.J., 2003. The diurnal cycle of rainfall and convective intensity according to three years of TRMM measurements. J.Cli. 16 (10), 1456–1475.
Padmakumari, B., Maheskumar, R., Anand, V., Axisa, D., 2017. Microphysical characteristics of convective clouds over ocean and land from aircraft observations. Atmos. Res. 195, 62–71.
Patel, P.N., Gautam, R., Michibata, T., Gadhavi, H., 2019. Strengthened Indian summer monsoon precipitation susceptibility linked to dust-induced ice cloud modification. Geophys. Res. Lett. 46, 8431–8441.
Pielke, R.A., 1974. A three-dimensional numerical model of the sea breezes over South Florida. Mon. Weather Rev. 102 (2), 115–139.
Radhakrishna, B., Rao, T.N., 2010. Differences in cyclonic raindrop size distribution from south-west to north-east monsoon season and from that of non-cyclonic rain. J. Geophys. Res. 115, D16205. https://doi.org/10.1029/2009JD013355.
Radhakrishna, B., Rao, T.N., Rao, D.N., Rao, N.P., Nakamura, K., Sharma, A.K., 2009. Spatial and seasonal variability of raindrop size distributions in Southeast India. J. Geophys. Res. 114, D04203. https://doi.org/10.1029/2008JD011226.
Rajeevan, M., Unnikrishnan, C.K., Bhate, J., Niranjan Kumar, K., Sreekala, P.P., 2012. Northeast monsoon over India: Variability and prediction. Meteorol. Appl. 19, 226–236. https://doi.org/10.1002/met.1322.
Ramanathan, V., Crutzen, P.J., Kiehl, J.T., Rosenfeld, D., 2001. Aerosols, climate, and the hydrological cycle. Science 294, 2119–2124.
Rao, T.N., Rao, D.N., Mohan, K., Raghavan, S., 2001. Classification of tropical precipitating systems and associated Z-R relations. J. Geophys. Res. 106, 17,699–17,711.
Rao, T.N., Radhakrishna, B., Nakamura, K., Rao, N.P., 2009. Differences in raindrop size distribution from southwest monsoon to northeast monsoon at Gadanki. Q. J. R. Meteorol. Soc. 135, 1630–1637.
Rauniyar, S.P., Walsh, K.J.E., 2013. Influence of ENSO on the diurnal cycle of rainfall over the Maritime Continent and Australia. J. Climatol. 26 (4), 1304–1321. https://doi.org/10.1175/JCLI-D-12-00124.1.
Rodwell, M.J., 2005. Monsoon internal dynamics. The global monsoon system: Research and forecast. In: World Meteorological Organization Report WMO/TD-1266, pp. 326–341. https://www.wmo.int/pages/prog/arep/tmrp/documents/global_monsoon_system_IWM3.pdf.
Rosenfeld, 2000. Suppression of rain and snow by urban air pollution. Science 287, 1793–1796.
Rosenfeld, D., Ulbrich, C.W., 2003. Cloud microphysical properties, processes, and rainfall estimation opportunities. Meteorol. Monogr. 30 (52), 237–258. https://doi.org/10.1175/0065-9401(2003)030%3C0237:CMPPAR%3E2.0.CO;2.
Seela, B.K., Janapati, J., Lin, P.-L., Reddy, K.K., Shirooka, R., Wang, P.K., 2017. A comparison study of summer season raindrop size distribution between Palau and Taiwan, two islands in western Pacific. J. Geophys. Res. 122, 11,787–11,805. https://doi.org/10.1002/2017JD026816.
Siew, J.H., Tangang, F.T., Juneng, L., 2014. Evaluation of CMIP5 coupled atmosphere–ocean general circulation models and projection of the Southeast Asian winter monsoon in the 21st century. Int. J. Climatol. 34, 2872–2884 (doi:10.1002/joc.3880).
Simpson, J., Keenan, T., Ferrier, B., Simpson, R., Holland, G., 1993. Cumulus mergers in the Maritime Continent region. Meteorl. Atmos. Phys. 51 (1–2), 73–99. https://doi.org/10.1007/BF01080881.
Sreekala, P.P., Rao, S.V.B., Rajeevan, M., 2012. Northeast monsoon rainfall variability over south peninsular India and its teleconnections. Theor. Appl. Climatol. 108, 73–83. https://doi.org/10.1007/s00704-011-0513-x.
Stout, G.E., Mueller, E.A., 1968. Survey ofrelationships between rainfall rate and radar reflectivity in the measurement of precipitation. J. Appl. Meteorol. 7, 465–474.
Sumesh, R.K., Resmi, E.A., Unnikrishnan, C.K., Jash, D., Sreekanth, T.S., Resmi, M.M., Rajeevan, K., Nita, S., Ramachandran, K.K., 2019. Microphysical aspects of tropical rainfall during Bright Band events at mid and high-altitude regions over Southern Western Ghats, India. Atmos. Res. 227, 178–197.
Tapiador, F.J., Checa, R., de Castro, M., 2010. An experiment to measure the spatial variability of rain drop size distribution using sixteen laser disdrometers. Geophys. Res. Lett. 37 (16) https://doi.org/10.1029/2010GL044120. L16803.
Thurai, M., Bringi, V.N., May, P.T., 2010. CPOL radar-derived drop size distribution statistics of stratiform and convective rain for two regimes in Darwin, Australia. J. Atmos. Ocean. Technol. 27 (5), 932–942. https://doi.org/10.1175/2010JTECHA1349.1.
Tokay, A., Bashor, P.G., 2010. An experimental study of smallscale variability of raindrop size distribution. J. Appl. Meteorol. Climatol. 49 (11), 2348–2365. https://doi.org/10.1175/2010JAMC2269.1.
Tokay, A., Short, D.A., 1996. Evidence from tropical raindrop spectra of the origin of rain from stratiform versus convective clouds. J. Appl. Meteorol. 35 (3), 355–371. https://doi.org/10.1175/1520-0450(1996)035<0355:EFTRSO>2.0.CO;2.

Uijlenhoet, R., Steiner, M., Smith, J.A., 2003. Variability of raindrop size distributions in a squall line and implications for radar rainfall estimation. J. Hydrometeorol. 4 (1), 43–61. https://doi.org/10.1175/1525-7541(2003)004,0043:VORSDI.2.0.CO;2.

Ulbrich, C.W., 1983. Natural variations in the analytical form of the raindrop size distribution. J. Climate Appl. Meteor 22, 1764–1775.

Ulbrich, C.W., Atlas, D., 2007. Microphysics of raindrop size spectra: Tropical continental and maritime storms. J. Appl. Meteorol. Climatol. 46 (11), 1777–1791. https://doi.org/10.1175/2007JAMC1649.1.

Vinoj, V., Rasch, P.J., Wang, H., Yoon, J.H., Ma, P.L., Landu, K., Singh, B., 2014. Short-term modulation of Indian summer monsoon rainfall by West Asian dust. Nat.Geosci. 7, 308–313.

Xiao, C., Yuan, W., Yu, R., 2018. Diurnal cycle of rainfall in amount, frequency, intensity, duration, and the seasonality over the UK. Int. J. Climatol. 38, 4967–4978.

Yang, G.Y., Slingo, J, 2001. The Diurnal Cycle in the Tropics. Mon. Wea. Rev. 129, 784–801.

Yang, S., Smith, E.A., 2008. Convective–stratiform precipitation variability at seasonal scale from 8 yr of TRMM observations: Implications for multiple modes of diurnal variability. J. Clim. 21, 4087–4114.

Yin, Y., Levin, Z., Reisin, T., Tzivion, S., 2000. Seeding convective clouds with hygroscopic flares: Numerical simulations using a cloud model with detailed microphysics. J. Appl. Meteorol. 39, 1460–1472.

Yuter, S.E., Houze, R.A., 1997. Measurements of raindrop size distributions over the Pacific warm pool and implications for Z–R relations. J. Appl. Meteorol. 36 (7), 847–867. https://doi.org/10.1175/1520-0450(1997)036<0847:MORSDO>2.0.CO;2.

Zubair, L., Ropelewski, C.F., 2006. The strengthening relationship between ENSO and northeast monsoon rainfall over Sri Lanka and southern India. J.Cli. 19, 1567–1575. https://doi.org/10.1175/JCLI3670.1.

Zwiebel, J., van Baelen, J., Anquetin, S., Pointin, Y., Boudevillain, B., 2015. Impacts of orography and rain intensity on rainfall structure. The case of the HyMeX IOP7a event. Q. J. Roy. Meteor. Soc. 142, 310–319. https://doi.org/10.1002/qj.2679.